

TOPIC 3

Fuel, Clad, Structural and Coolant Materials

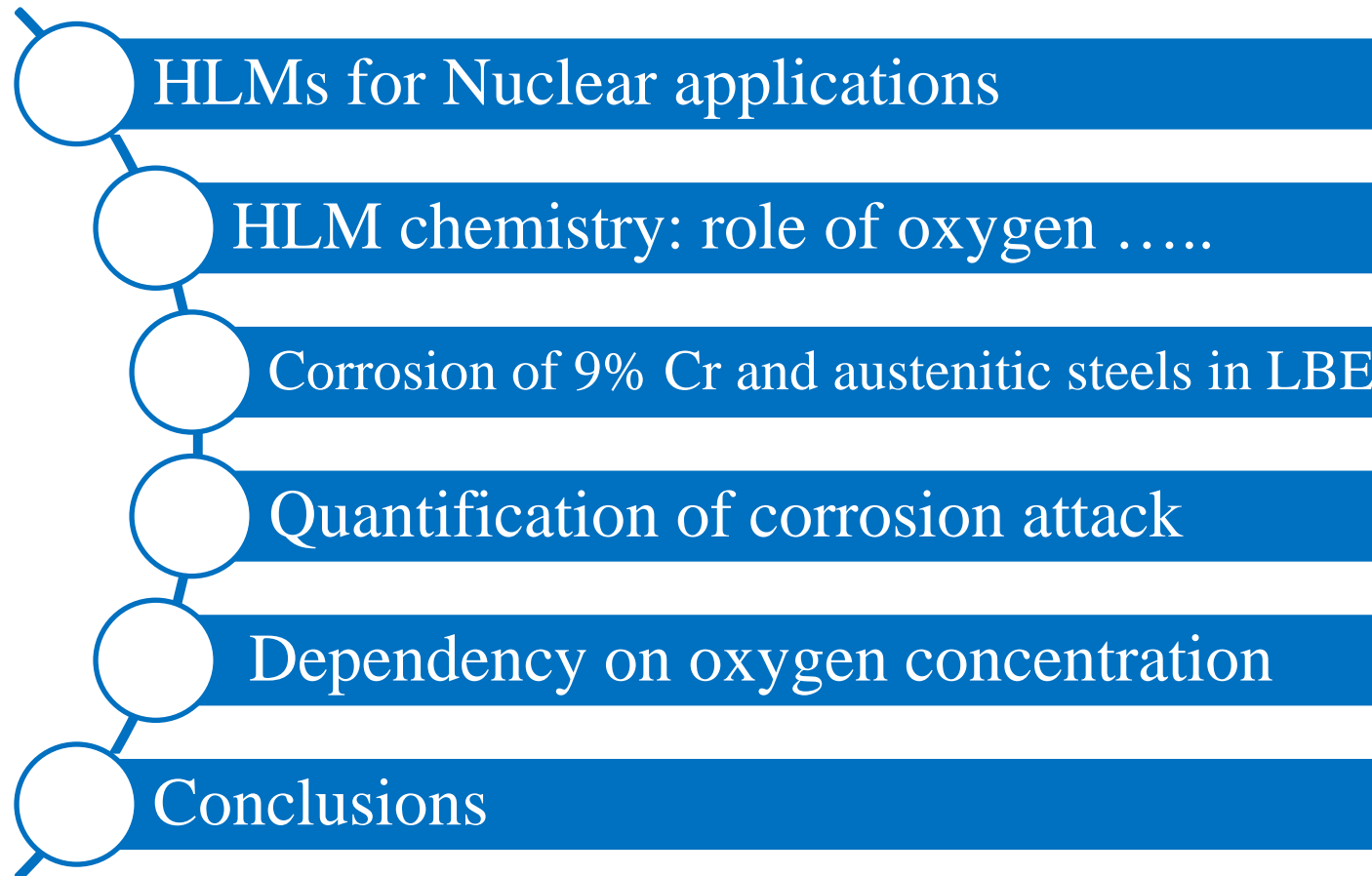
Sub topic 3.3:

Compatibility of Fast Reactor Structural Materials with Liquid Metal Coolants (Part 2)

Juergen Konys

Karlsruhe Institute of Technology

juergen.konys@kit.edu



FJOH 2016 Heavy Liquid Metals for Energy Applications

❑ Why: Favourable properties of liquid metals

- ❑ High thermal conductivity and boiling point
- ❑ Reasonably low dynamic viscosity
- ❑ Some show minimum interaction with neutrons (e.g., sodium and lead)
- ❑ Heavy liquid metals release neutrons under proton irradiation (e.g., mercury, lead and bismuth)

→ Efficient heat transfer medium/
coolant for **thermal energy conversion**

→ Essential for **fast neutron reactors**

→ Allows for sub-critical nuclear fuel in
a **proton-accelerator driven system (ADS)**



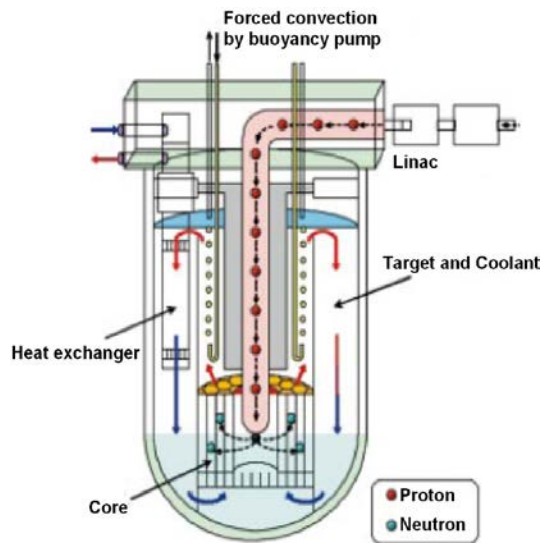
❑ But: Compatibility issue between liquid metals and e.g. steels

- ❑ Major steel elements are (very) soluble in liquid metals (Fe, Cr, Ni)
- ❑ Formation of intermetallic phases (Sn)
- ❑ Degradation of mechanical properties
 - Prominent issue for lead alloys, especially lead-bismuth eutectic (LBE)

FJOH 2016 Some Specific Properties of Liquid Metals

		UNIT	Pb ⁴⁵ Bi ⁵⁵	Pb-16Li	SODIUM	WATER
Melting Point at 0.1 MPa		[°C]	125	235	97.8	0
Boiling Point at 0.1 MPa		[°C]	2516	1600	881	100
			300°C	300°C	300°C	25°C
Density	ρ	[kg/m ³]	10325	9988	880	1000
Heat Capacity	c_p	[J/(kgK)]	146.33	200.22	1298	4180
Kinematic Viscosity	ν	[m ² /s] · 10 ⁻⁷	1.754	1.3	4	9.1
Heat Conductivity	λ	[W/(m K)]	12.68	45.2	77.1	0.6
Electric Conductivity	σ_{el}	[A/(V m)] · 10 ⁵	8.428	12.67	55.5	2 · 10 ⁻⁴ (tap)
Thermal Expansion Coefficient	α	[K ⁻¹] · 10 ⁻⁶	6.7	41.2	24.2	6
Surface Tension	σ	[N/m] · 10 ⁻³	410	430	175	52 (tap)

FJOH 2016 Heavy Liquid Metal-cooled Nuclear Reactors

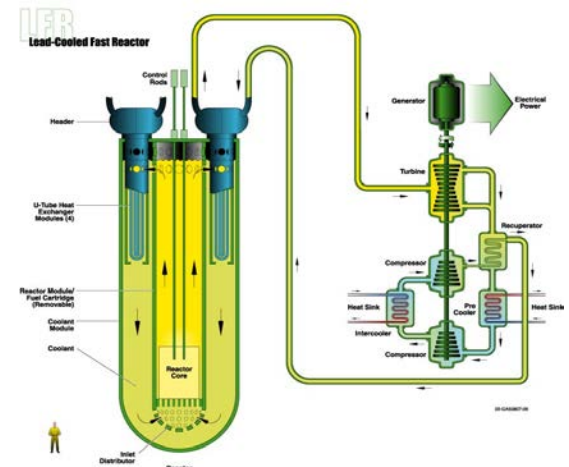


Accelerator Driven (Subcritical) System (ADS)

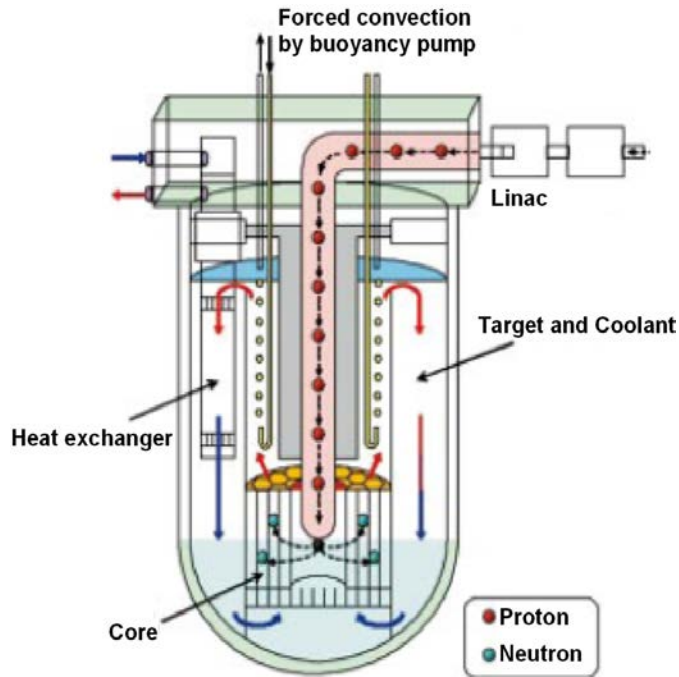
- Transmutation of long-lived radioactive isotopes in nuclear waste
- Power generation (Energy Amplifier)
- Liquid lead (Pb) or lead-bismuth eutectic (LBE) as spallation target and primary coolant
- Maximum temperature, typically
 - 450 – 500°C for regular operation
 - Periodically 550°C (according to plant design)

Lead-Cooled Fast Reactor (LFR)

- One of the concepts for the 4th generation of nuclear power plants (Gen-IV)
- In the long-term, Pb as primary coolant at maximum ca. 800°C
- Short- to mid-term: Pb- or LBE-cooled at 450 – 550°C



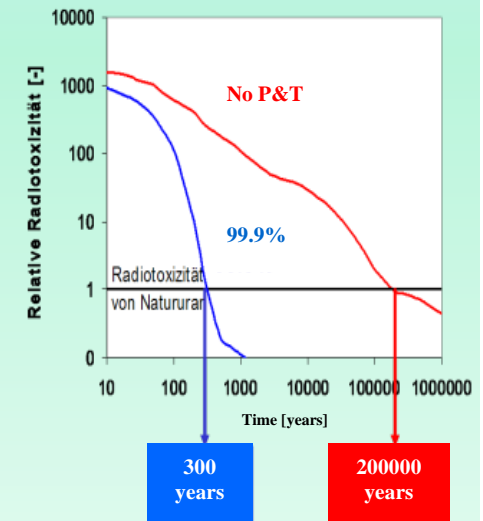
FJOH 2016 Heavy Liquid Metal-cooled Nuclear Reactors



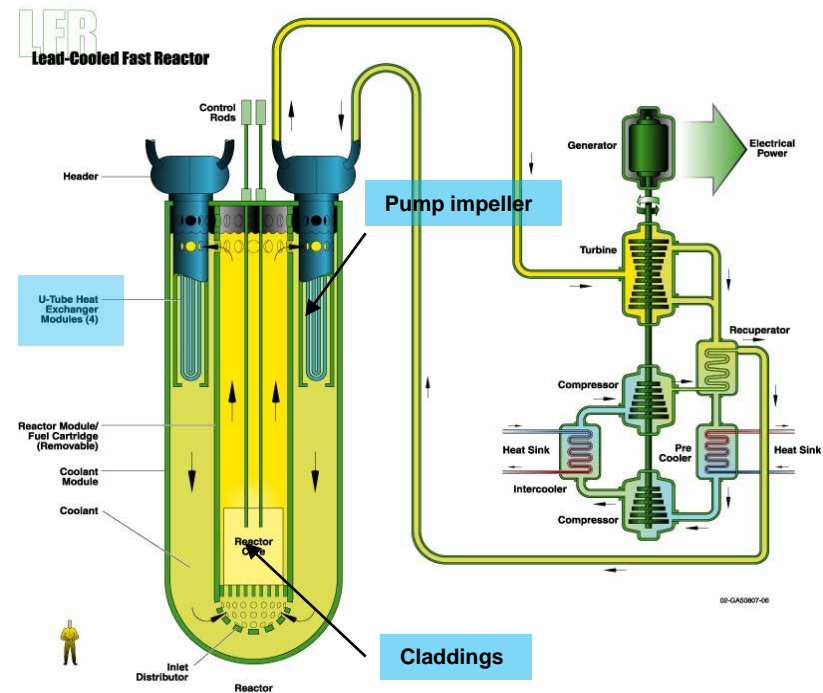
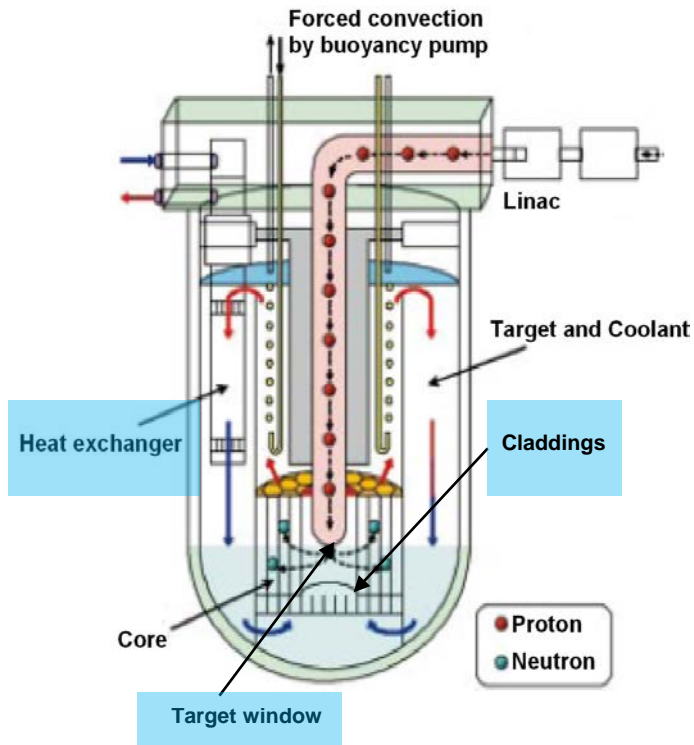
Reduction of high-level nuclear waste

	No. NPPs		Burned Fuel (t)	
	No.	Electricity gen.	Accumulated	Per year
Worldwide	438	16%	220 000	7 000
EU	145	35%	34 500	2 500
Germany	19	30%	8 400	450

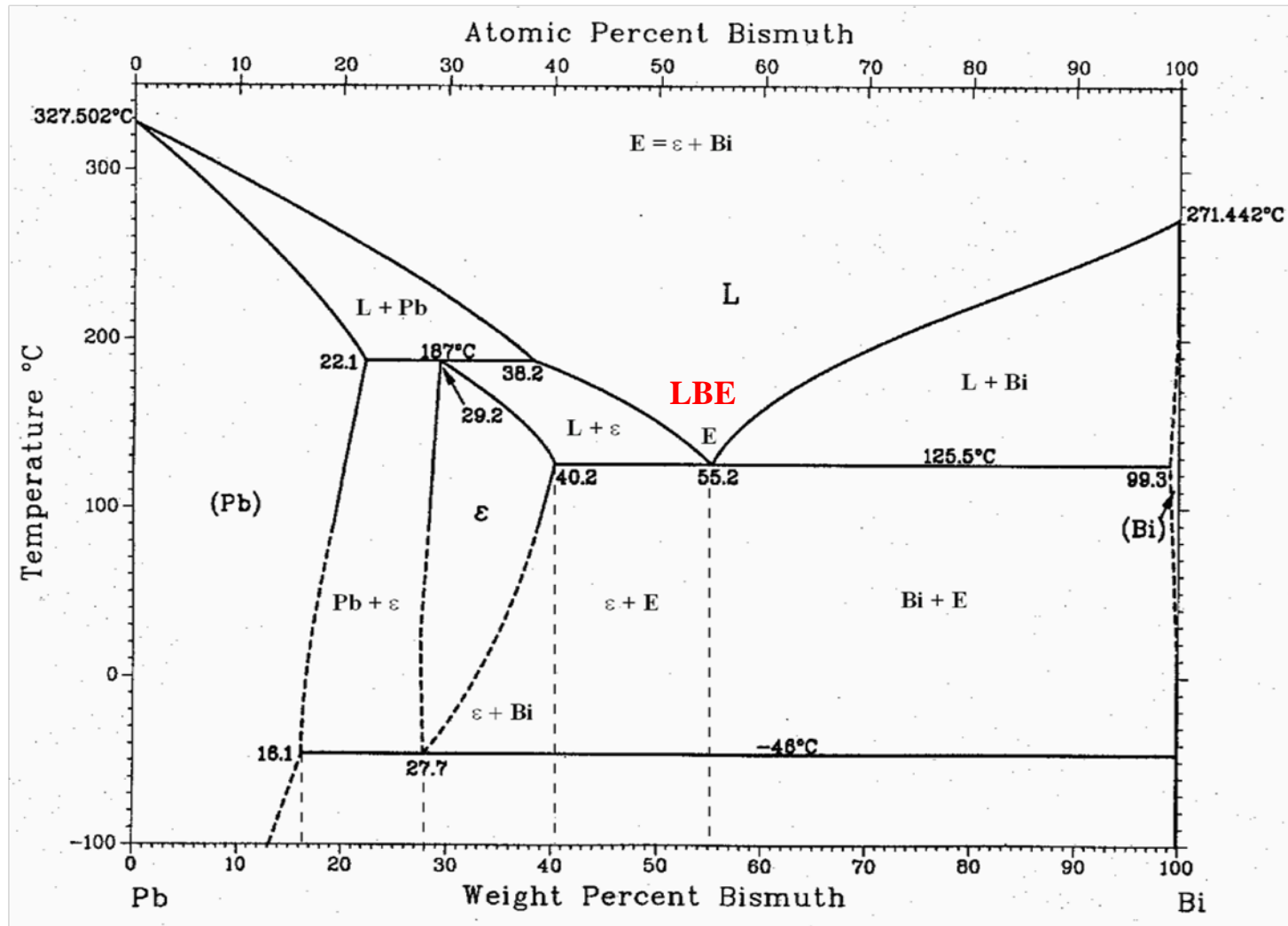
Influence of partitioning rate of Pu and MA on the radiotoxicity of burned fuel



Critical Components of Heavy Liquid Metal-cooled Nuclear Reactors/Systems



FJOH 2016 Phase Diagram Lead – Bismuth Eutectic (LBE)



FJOH 2016 Heavy Liquid Metal (HLM) – Steel Interactions

□ Corrosion

- Solution of steel elements with preferential (Ni, Cr) rather than general removal
- Surface recession and/or development of a near-surface depletion zone
- Infiltration of the depletion zone by the liquid metal
- Formation of intermetallic phases on the steel surface or in a near-surface zone inside the steel

Observed on the μm -scale, accessible by light-optical microscopy (LOM), scanning-electron microscopy (SEM), energy-dispersive X-ray spectroscopy (EDX), X-ray diffraction (XRD) ...

Liquid-metal embrittlement (LME), softening, oxidation..

□ Degradation of mechanical properties

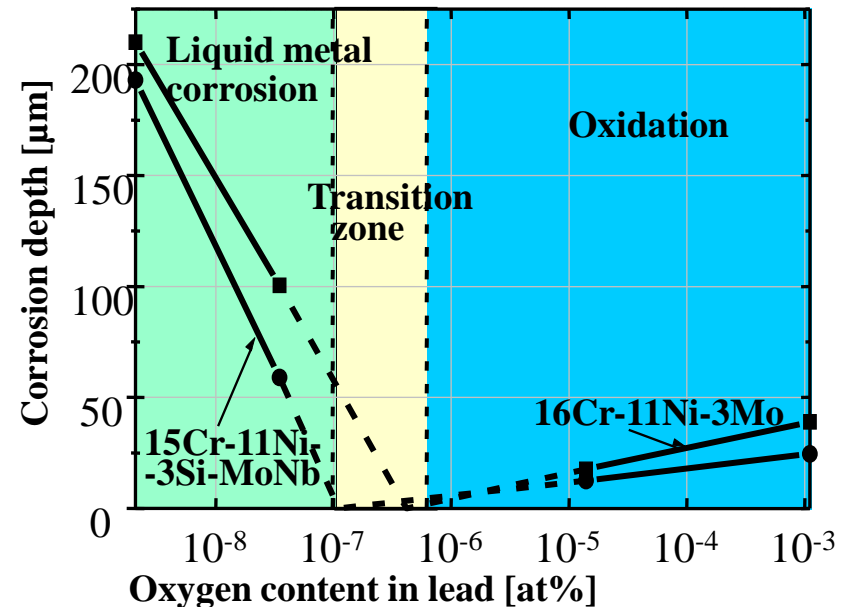
- Damage accumulation at the surface due to corrosion
- Or arising from phenomena below the μm -scale:
 - Adsorption of liquid-metal elements
 - Subsequent processes affecting near-surface defects (dislocations, grain boundaries, cracks)
- Quantification by tensile, slow-strain rate, creep, fatigue, fracture-toughness tests performed either in or after exposure to the liquid metal

FJOH 2016 Impact of Oxygen on Steel Corrosion in HLMS

- ❑ **“Absence” of oxygen (Pb-16Li)**
 - Chemical oxygen potential too low for remarkable interactions with steel elements
 - Steel elements dissolve in the liquid metal
 - Absorption of liquid metal constituents by the steel
 - (▪ Formation of intermetallic phases)

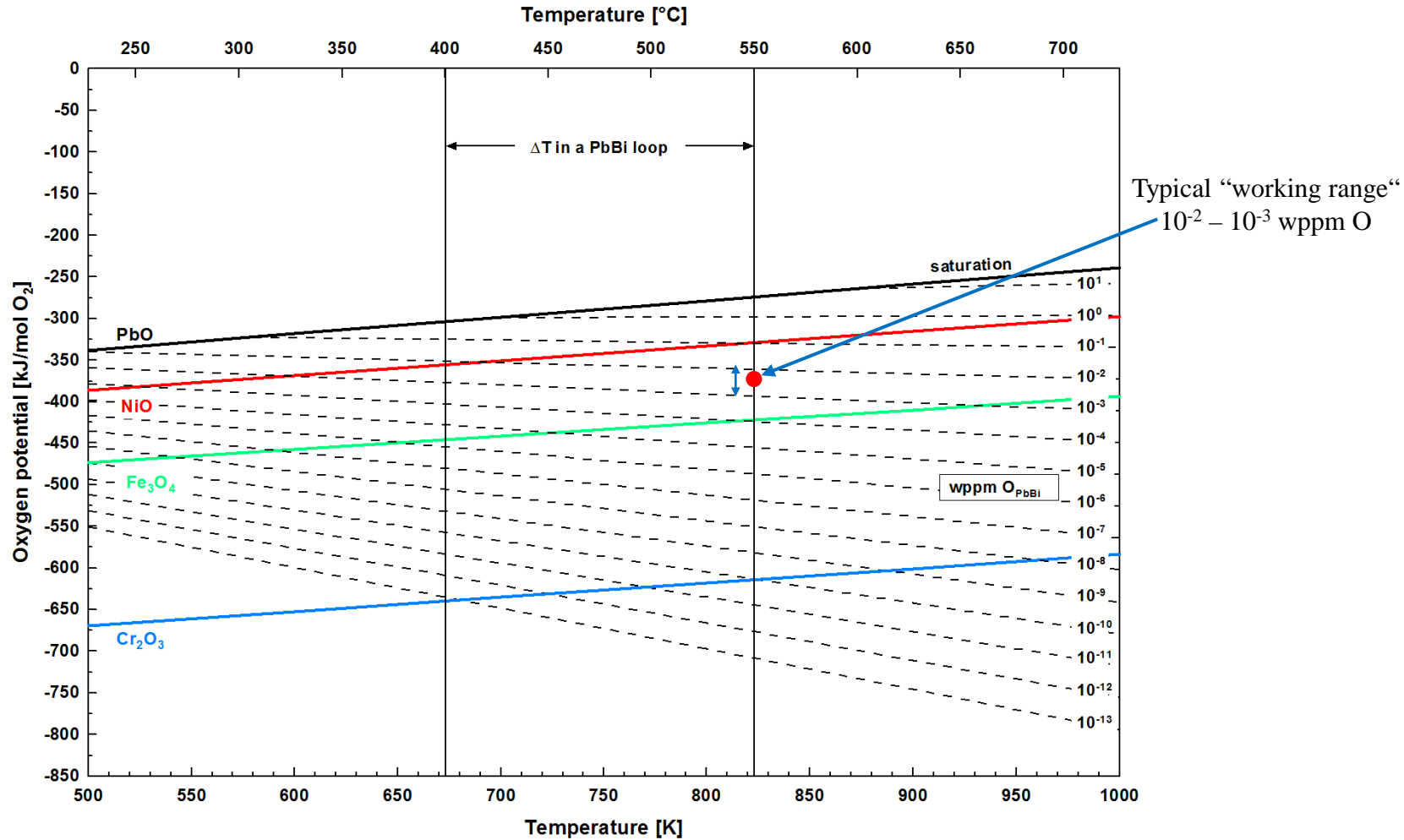
- ❑ **Low-oxygen conditions (Pb, LBE)**
 - Solid oxides of steel elements are stable
 - But, amount of oxides formed too small for a continuous surface layer
 - Concentration gradients that promote solution of steel elements may develop in the liquid metal

- ❑ **High-oxygen conditions (Pb, LBE)**
 - Solid oxides of steel elements form a continuous surface layer
 - Solution of steel elements still possible, but only after diffusion through solid oxide



- ➔ Transition from solution-based to oxidation-based corrosion with increasing oxygen concentration
- ➔ Continuous oxide layer is the goal of deliberate oxygen addition (Pb, LBE)
- ➔ Locally low-oxygen conditions even when oxygen concentration in the bulk of the liquid metal is high

FJOH 2016 Oxygen Chemistry: Oxygen Potentials in HLMs



FJOH 2016 Components of an Oxygen Control System

Sensors for on-line monitoring

Electrochemical oxygen monitoring

- Solid electrolyte on the basis of yttria-stabilized zirconia (YSZ)
- Metal/metal-oxide or Pt/gas reference electrode

Issues to be addressed (in general)

- Compatibility with the use in Pb alloys (YSZ/steel joint)
- Accuracy
- Long-term reliability

Licensing for nuclear application

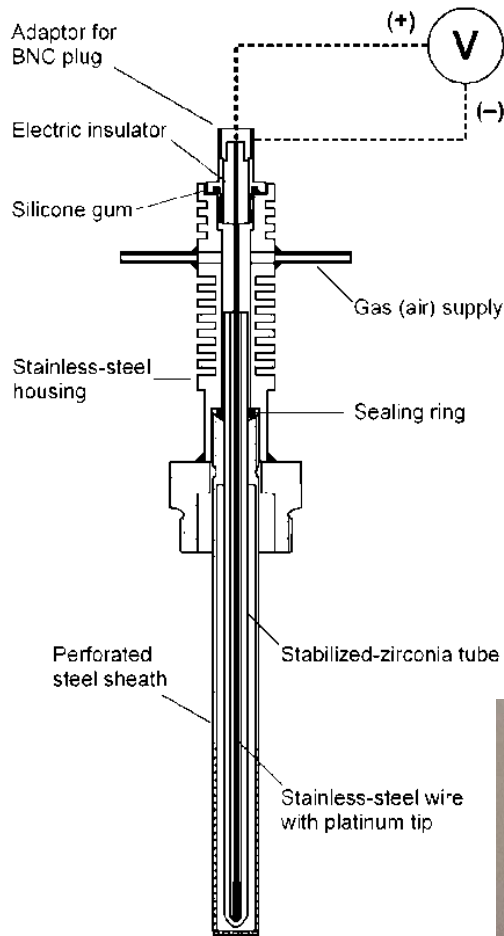
- Structural stability of the YSZ product used
- Risk of contamination in case of electrolyte cracking

Oxygen-transfer device(s)

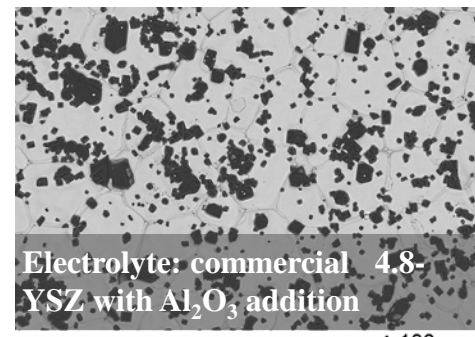
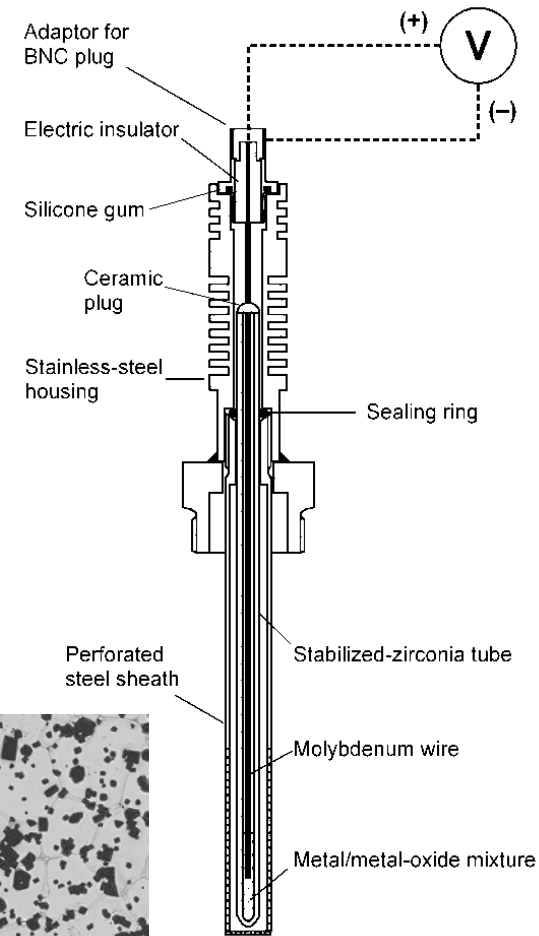
“Classic“ mass transfer across the interface between oxygen source/sink and the liquid metal

Type	Oxygen source	Oxygen sink
Solid-liquid	PbO	(less noble metals)
Gas-liquid	Ar, H ₂ O, air	Ar-H ₂

Long-term experience from operating experimental facilities for testing materials (steels) in oxygen-containing Pb alloys exists



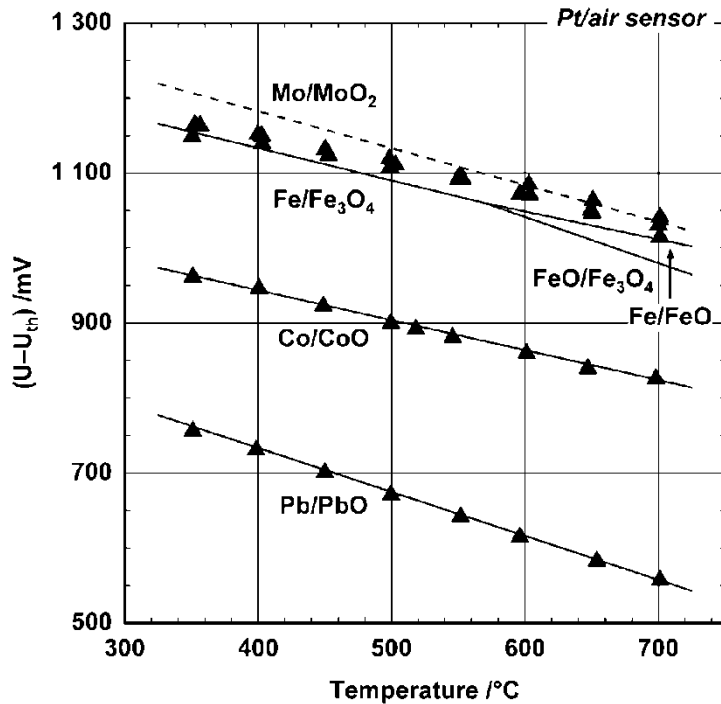
- Long electrolyte tube ($\text{\O} 6 \times 255 \text{ mm}$)
- Polymer sealing ring in sufficient distance from the liquid metal
- Cooling fins for reducing the thermal load on the sealing ring
- Steel sheath for protecting the electrolyte from shear forces, serving as electric lead on the liquid-metal side
- Reference electrodes
 - (Steel)Pt/air
 - (Mo)Bi/Bi₂O₃



Electrolyte: commercial 4.8-YSZ with Al₂O₃ addition

100 μm

Accuracy of measurement resulting from comparison with metal/metal-oxide equilibria adjusted in LBE



Fe oxide equilibria

- Stepwise cooling or heating
- Ar-15% H₂ bubbling continuously through the LBE (5 ml/min) or quasi-stagnant
- Oxygen potentials move from Fe-oxide to Mo/MoO₂ equilibrium with temperature variation (Mo comes from wire submerged in the LBE)

Co/CoO

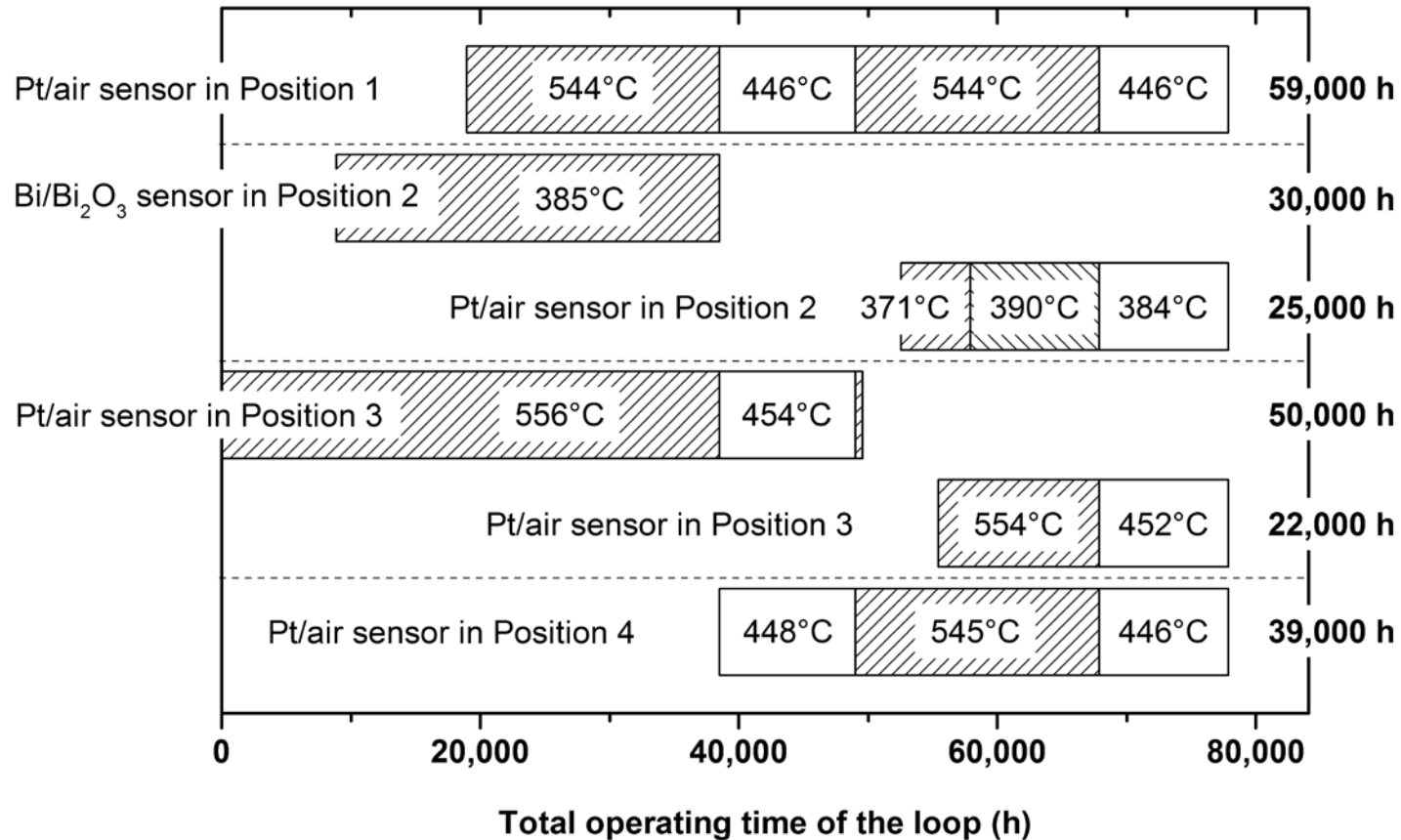
- Stepwise cooling
- Ar 5.0 bubbling continuously through the LBE (5 ml/min)
- Periodically addition of air (5 ml/min) at 700 and 650°C
- Maximum deviation from theoretical prediction < 6 mV

Pb/PbO

- Stepwise cooling
- Ar 5.0 bubbling continuously through the LBE (5 ml/min)
- Maximum deviation from theoretical prediction < 4 mV

Accumulated operating time of oxygen sensors in the **CORRIDA loop**

Currently + 10000 h



CORRIDA

Testing characteristics

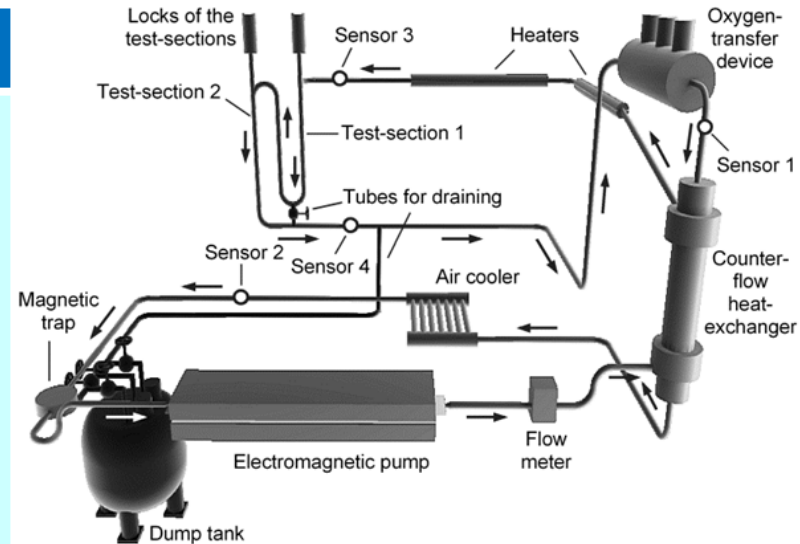
Exposure to flowing LBE, typically 2 m/s. **1000 kg circulating LBE** (5.3 kg/s). Several steel samples simultaneously exposed in vertical test-sections. Oxygen control via gas with variable oxygen partial pressure. Large internal steel surface in contact with the liquid metal. Temperature difference along the loop of ~100–150°C.

Sample geometry

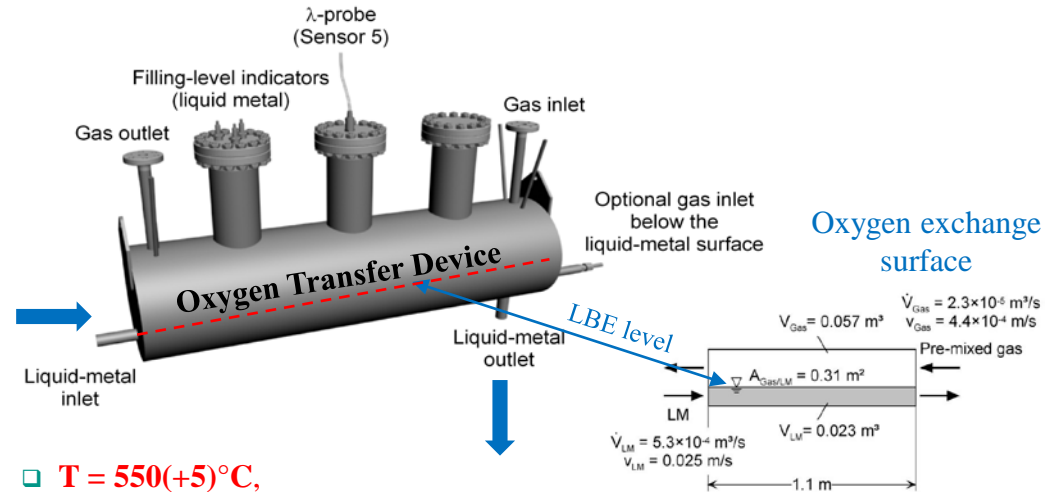
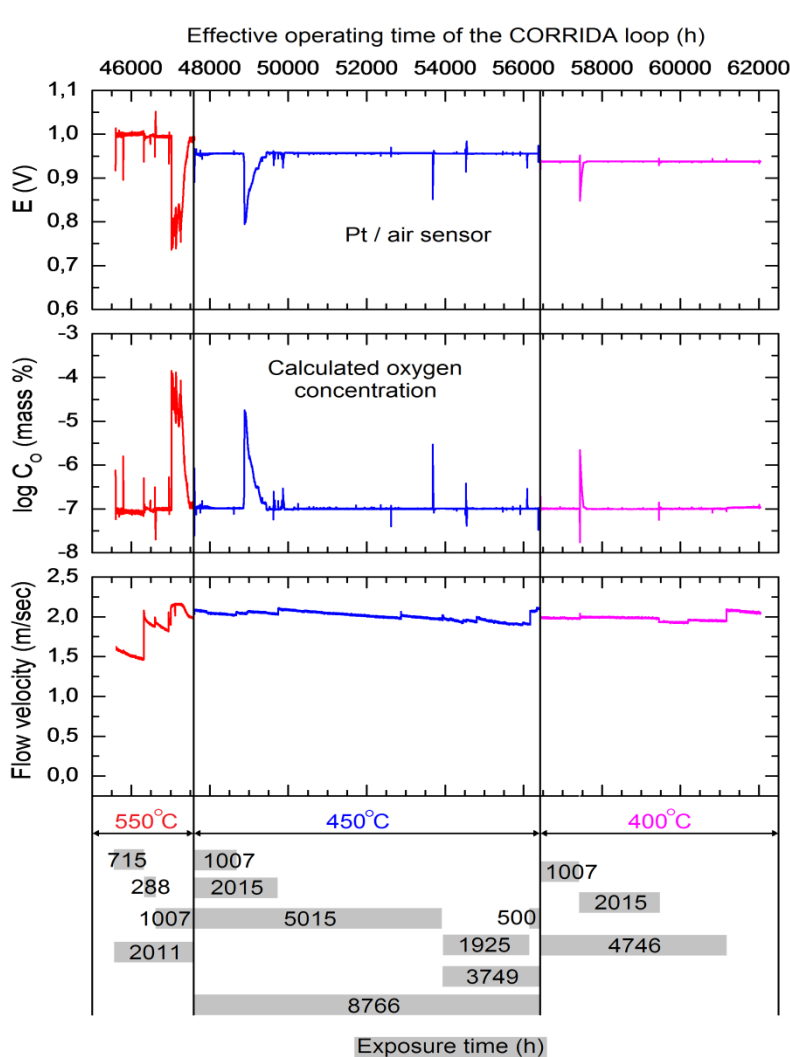
Typically, cylindrical specimen with 7.5 cm² exposed to liquid metal.

Determination of oxygen content

Four potentiometric oxygen sensors distributed along the loop.



Constructed and operated since mid 2003



□ **T = 550(+5)°C,**

$T_{\min} \approx 385^\circ\text{C}$, $c_{\text{O}} = 10^{-7}$ mass%, excursion to 10^{-4} – 10^{-5} mass% O,

$v = 2(+/-0.2)$ m/s, initially 1.5–1.6 m/s,

$t = 288; 715; 1007; 2011$ h

□ **T = 450(+5)°C,**

$T_{\min} \approx 350^\circ\text{C}$, $c_{\text{O}} = 10^{-7}$ mass%, excursion to 10^{-5} mass% O

$v = 2(+/-0.2)$ m/s,

$t = 500; 1007; 1925; 2015; 3749; 5015; 8766$ h

□ **T = 400(+5)°C,**

$T_{\min} \approx 350^\circ\text{C}$, $c_{\text{O}} = 10^{-7}$ mass%,

$v = 2(+/-0.2)$ m/s,

$t = 1007; 2015; 4746$ h; still continuing up to 10,000h

FJOH 2016 Relevant 9% Cr Steels for ADS and LFR

Concentration (in wt%) of alloying elements other than Fe

	Cr	Mo	W	V	Nb	Ta	Y	Mn	Ni	Si	C
T91-A	9.44	0.850	<0.003	0.196	0.072	n.a.	n.a.	0.588	0.100	0.272	0.075
T91-B	8.99	0.89	0.01	0.21	0.06	n.a.	n.a.	0.38	0.11	0.22	0.1025
E911*	8.50–	0.90–	0.90–	0.18–	0.060–	–	–	0.30–	0.10–	0.10–	0.09–
	9.50	1.10	1.10	0.25	0.100	–	–	0.60	0.40	0.50	0.13
EF-ODS-A	9.40	0.0040	1.10	0.185	n.a.	0.08	0.297 [†]	0.418	0.0670	0.115	0.072
EF-ODS-B	8.92	0.0037	1.11	0.185	n.a.	0.078	0.192 [†]	0.408	0.0544	0.111	0.067

* Nominal composition

[†] In the form of yttria (Y₂O₃)

↑
Elements besides Cr that are likely to improve oxidation performance

Microstructure

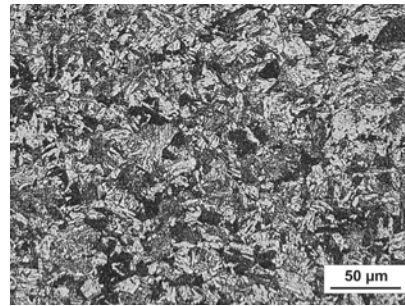
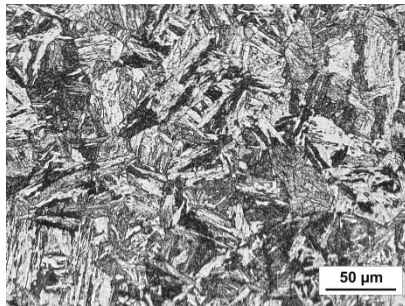
Fully martensitic:

E911, T91-A

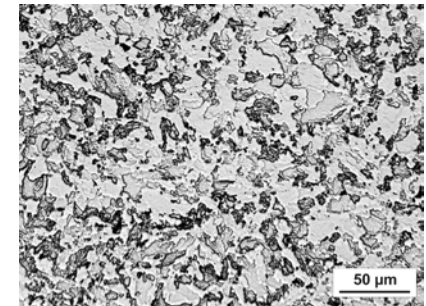
T91-B

Grain size

EUROFER



Mainly ferritic: ODS-A, ODS-B

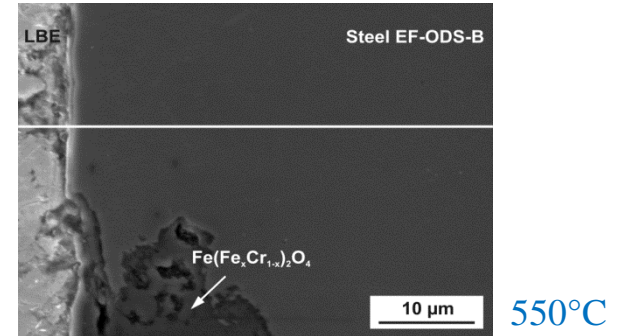


FJOH 2016 Corrosion Phenomena of 9% Cr Steels in LBE

Protective scaling

$T = 450 - 550^\circ\text{C}$, $v = 2 \text{ m/s}$, 10^{-6} wt\% O

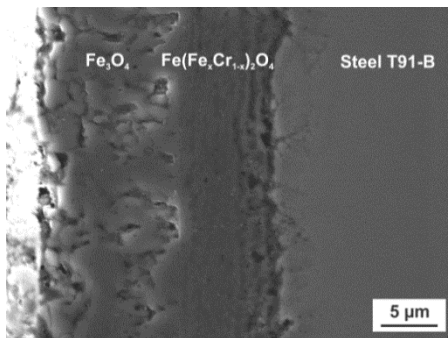
- Thin Cr- (Si-) rich oxide scale (thickness $\sim 1 \mu\text{m}$ or less)
- Promoted by high Cr content, fine-grained structure, dispersed Y_2O_3 ...
- Favourable situation with respect to minimum material loss, but generally not of long duration (locally)



↓ Scale failure at high local c_{O} (?)

↓ Scale failure at low local c_{O} (?)

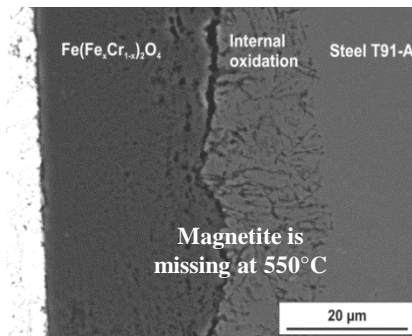
Accelerated oxidation



450°C

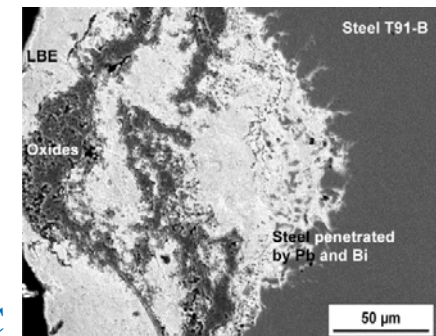
550°C

- Typical and, finally, the general corrosion process for 9% Cr steel



Solution-based corrosion

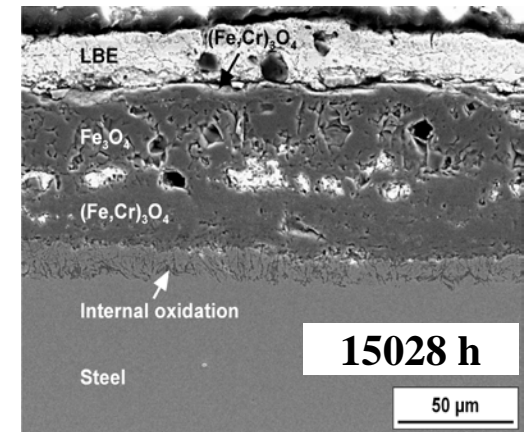
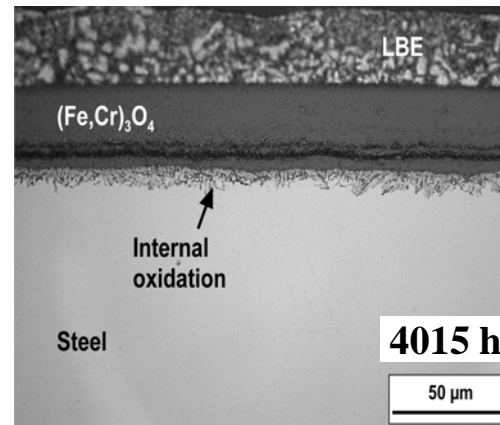
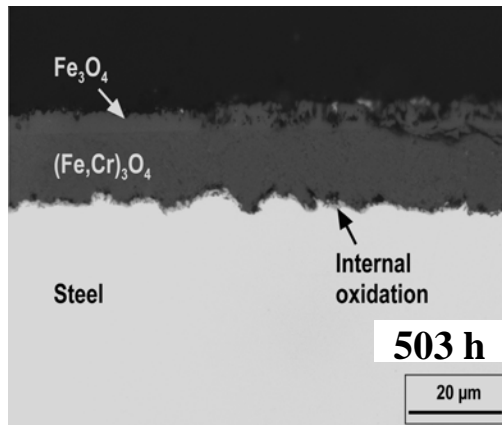
- Steel elements first dissolve but may re-precipitate in the form of oxides
- Intermittent solution participates in accelerated oxidation processes or solution outweighs oxidation
- Substantial loss of material!



550°C

FJOH 2016 Corrosion Phenomena of 9% Cr Steels in LBE

$T = 550^{\circ}\text{C}$, $v = 2 \text{ m/s}$, $1.6 \times 10^{-6} \text{ wt\% O}$

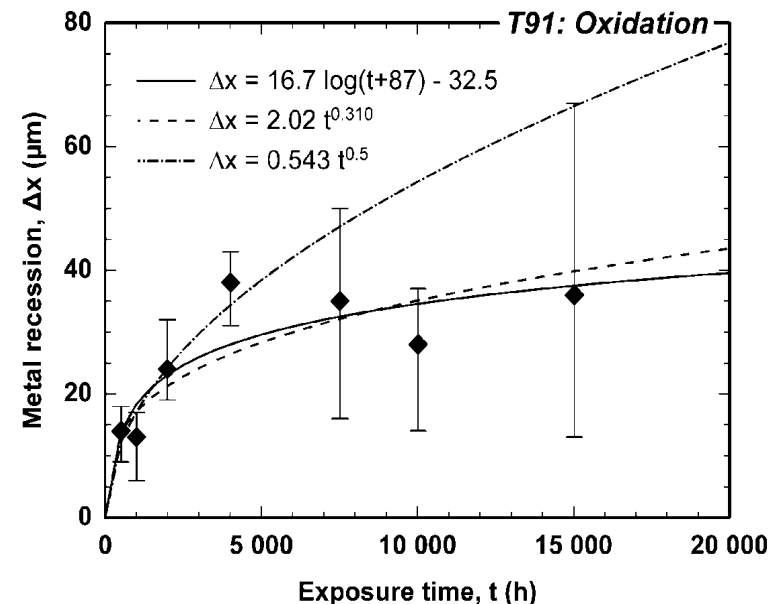


- Oxidation
- Oxide scale consists of
 - Magnetite (Fe_3O_4)
 - Cr-deficient spinel ($\text{Fe}(\text{Fe}_x\text{Cr}_{1-x})_2\text{O}_4$)
 - Internal Oxidation Zone (IOZ)
- Magnetite is mostly missing, i. e., Fe is partially dissolved in the liquid metal (or eroded after Fe_3O_4 formation?)
- Inclusions of Pb and Bi inside the scale, especially after long exposure times

FJOH 2016 Corrosion Phenomena of 9% Cr Steels in LBE

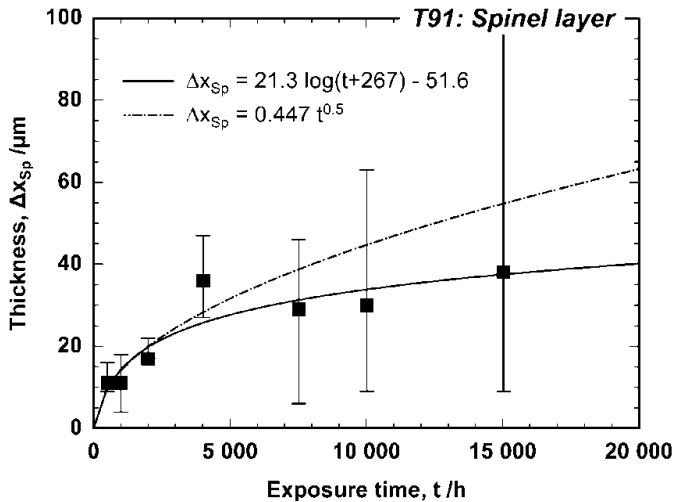
$T = 550^{\circ}\text{C}$, $v = 2 \text{ m/s}$, $1.6 \times 10^{-6} \text{ wt\% O}$

- Metal recession (loss of cross-section)
- Compromises the structural integrity of plant components
- Determined from measurements in the LOM (generally six measurements per investigated cross-section)
- Includes internal oxidation
- Local variation significantly increases with increasing exposure time
- Optimistic prediction: 50–70 μm after 100,000 h
- Worst-case: 100 μm after 4 years



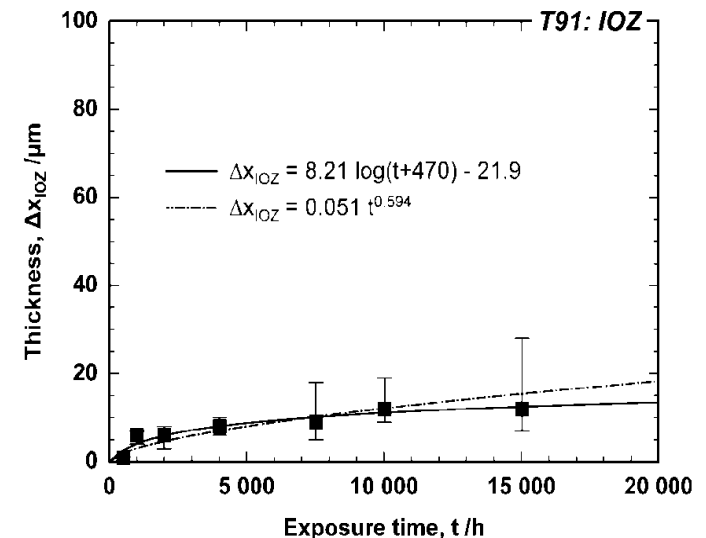
FJOH 2016 Corrosion Phenomena of 9% Cr Steels in LBE

$T = 550^{\circ}\text{C}$, $v = 2 \text{ m/s}$, $1.6 \times 10^{-6} \text{ wt\% O}$



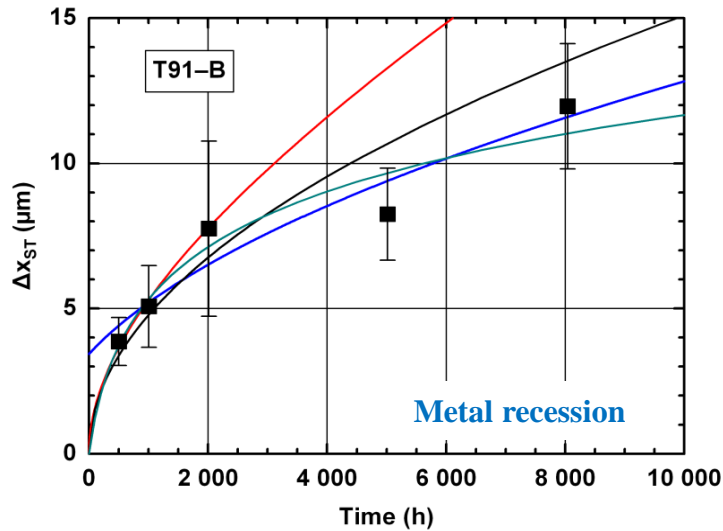
- Thickness of different layers of the oxide scale
- May affect heat transfer in the case of thermally-loaded plant components
- Generally twelve measurements per investigated cross-section
- Thickness of spinel layer significantly varies locally with increasing exposure time
- Average thickness of the spinel layer is in the order of the metal recession

Fe flux into the LBE can be estimated from the spinel layer thickness



FJOH 2016 Corrosion Phenomena of 9% Cr Steels in LBE

$T = 450^{\circ}\text{C}$, $v = 2 \text{ m/s}$, $1.6 \times 10^{-6} \text{ wt\% O}$



Parabolic:	$\Delta x^2 = k_2 t$
Parabolic after faster kinetics:	$\Delta x^2 = k_2 t + C_2$
Paralinear model of oxide scale growth	
Logarithmic:	$\Delta x = k_{\log} (t + t_0) + C_{\log}$

Exposure time (years)	1	5	10
T91-A → Upper limit of Cr content specified for T9			
$\Delta x_M (\mu\text{m})$	10	13 – 22	13 – 31
$\Delta x_{SP} (\mu\text{m})$	7	8 – 14	8 – 20
$\Delta x_{ST} (\mu\text{m})$	9	20	28
T91-B → Lower limit of Cr content specified for T91			
$\Delta x_M (\mu\text{m})$	12	15 – 26	15 – 36
$\Delta x_{SP} (\mu\text{m})$	8	10 – 16	10 – 23
$\Delta x_{ST} (\mu\text{m})$	12	26	37

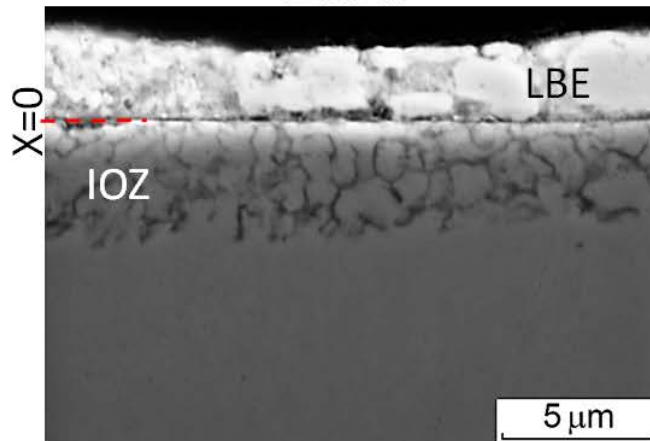
FJOH 2016 Corrosion Phenomena of 9% Cr Steels in LBE

T = 550°C, v = 2 m/s, 10⁻⁷ wt% O

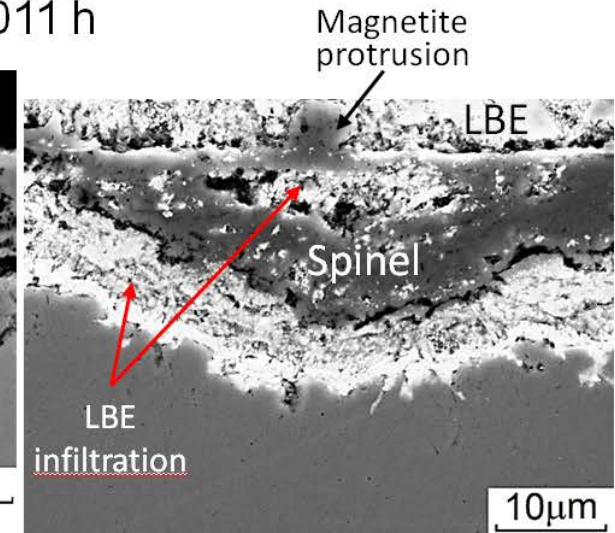
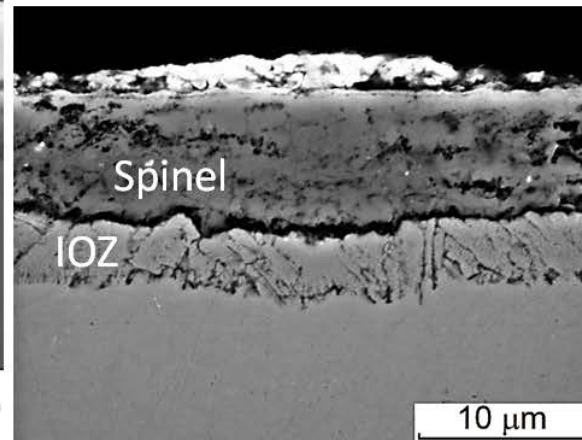
□ Accelerated oxidation

- Starts with internal oxidation
 - Spinel formation follows internal oxidation
 - Consumes outer part of the internal oxidation zone (IOZ) that may still grow at the IOZ/steel interface
 - General aspect of accelerated oxidation at 550°C, not only at low oxygen concentration of the LBE
- Outer magnetite layer is missing
 - Some magnetite protrusions after excursion to higher c_O
 - Corresponds to previous observations at 550°C/10⁻⁶ mass% O
 - Fe dissolves at the spinel surface rather than forming magnetite

288 h



2011 h



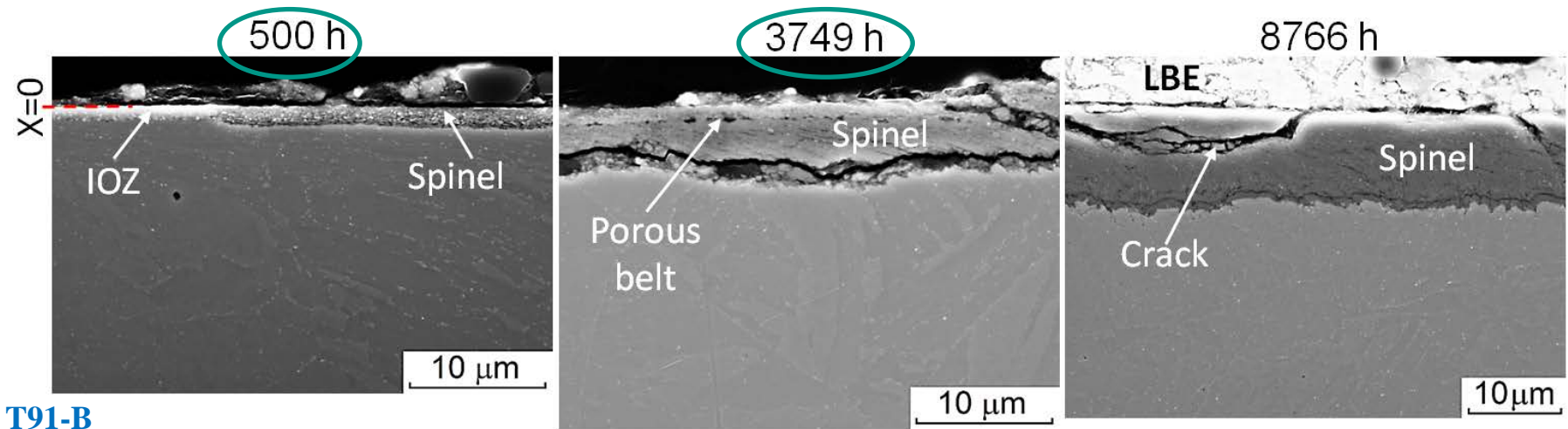
T91-A

FJOH 2016 Corrosion Phenomena of 9% Cr Steels in LBE

T = 450°C, v = 2 m/s, 10⁻⁷ wt% O

□ Accelerated oxidation

- Internal oxidation less pronounced than at 550°C
- In general, only spinel layer observed
- Pores in the outer part due to Fe diffusion towards the spinel surface
- No magnetite at constantly 10⁻⁷ mass% O
- Threshold oxygen concentration for magnetite formation between 10⁻⁷ and 10⁻⁶ mass% O at 450°C



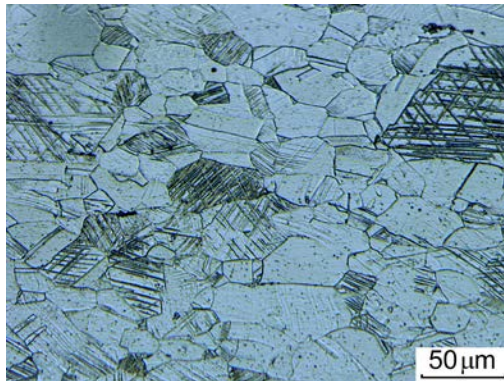
T91-B

FJOH 2016 Relevant Austenitic Steels for ADS and LFR

Concentration (in wt%) of alloying elements other than Fe

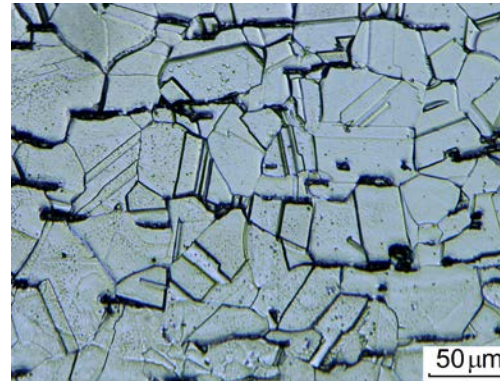
Austenitic steels	Cr	Ni	Mo	Mn	Si	Cu	V	W	Al	Ti	C	N	P	S	B
316L	16.73	9.97	2.05	1.81	0.67	0.23	0.07	0.02	0.018	-	0.019	0.029	0.032	0.0035	-
1.4970	15.95	15.4	1.2	1.49	0.52	0.026	0.036	< 0.005	0.023	0.44	0.1	0.009	< 0.01	0.0036	< 0.01
1.4571 (316-Ti)	17.50	12	2.0	2.0	1.0	-	-	-	-	0.70	0.08	-	0.045	0.015	-

1.4970 (15-15 Cr Ni)



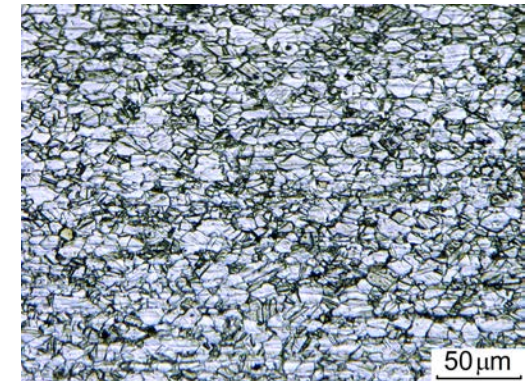
- HV₃₀ = 253;
- Grain size ranged from 20 to 65 μm;
- Intersecting deformation twins.

316L



- HV₃₀ = 132;
- Grain size averaged 50 μm (G 5.5);
- Annealing twins.

1.4571 (316-Ti)



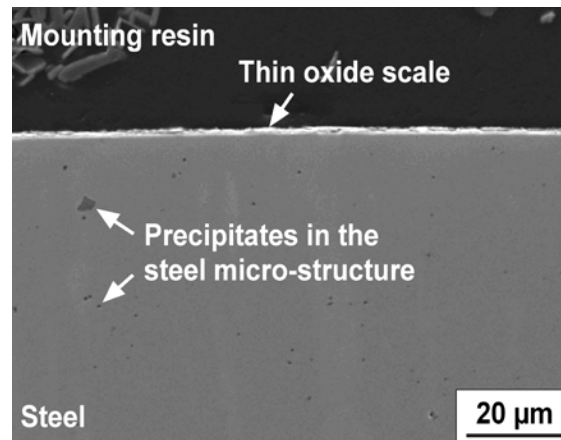
- HV₃₀ = 245;
- Grain size averaged 15 μm (G 9.5).

FJOH 2016 Corrosion Phenomena of Austenitic Steels in LBE

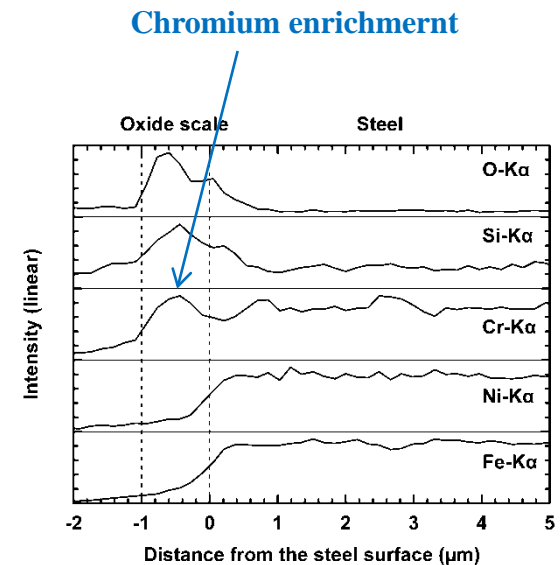
$T = 550^{\circ}\text{C}$, $v = 2 \text{ m/s}$, 10^{-6} wt\% O

Protective scaling

- Thin oxide scale ($< 1 \mu\text{m}$) consisting of Cr- or Si-rich oxide layers
- Might have evolved from thin films already existing on the steel surface before exposure
- Similar to the scale formed by pre-oxidation in dry gas (Ar)
- Locally long-lasting phenomenon on specimens exposed at $450/550^{\circ}\text{C}$, 10^{-6} wt\% O in the test-sections of the loop
- *Not observed on tube samples taken from the hot leg of the loop; effect of long exposure time and varying c_{O} (?)*



1.4571 specimen exposed in the test sections after 3,495 h at 550°C and $c_{\text{O}} \approx 10^{-6} \text{ wt\%}$



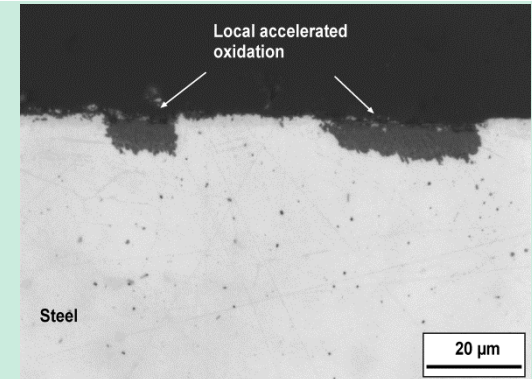
FJOH 2016 Corrosion Phenomena of Austenitic Steels in LBE

$T = 550^{\circ}\text{C}$, $v = 2 \text{ m/s}$, 10^{-6} wt\% O

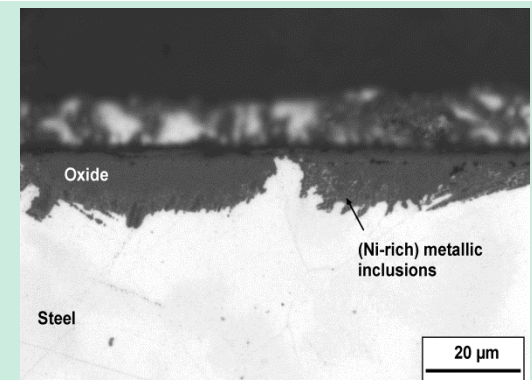
Accelerated oxidation

- Starts locally where the thin oxide scale lost integrity or did not form
- Formation of $\text{Fe}(\text{Fe}_x\text{Cr}_{1-x})_2\text{O}_4$, Fe_3O_4 and an internal oxidation zone; the latter two depending on oxygen content, temperature (or flow velocity)
- The thicker scale spreads on the steel surface with time and becomes partially continuous
- Varying c_{O} (mostly lower than 10^{-6} mass\%) seems to promote accelerated oxidation

1.4571 specimens in the test sections of the loop:



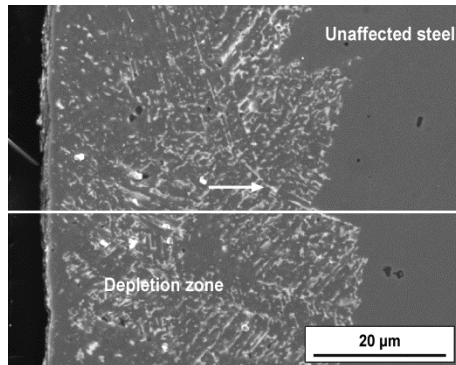
After exposure for 3,495 h at 550°C and $c_{\text{O}} \approx 10^{-6} \text{ wt\%}$



After exposure for 10,006 h at 550°C and varying c_{O}

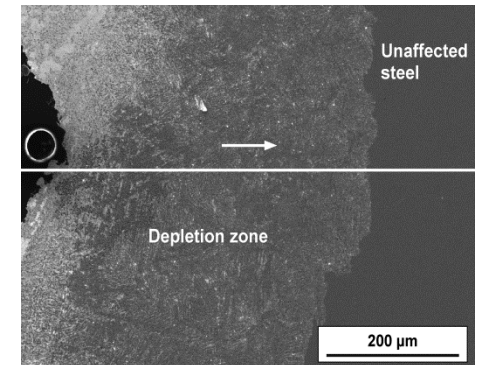
FJOH 2016 Corrosion Phenomena of Austenitic Steels in LBE

1.4571 after exposure for 5,012 h at 550°C and $c_O \approx 10^{-6}$ wt%



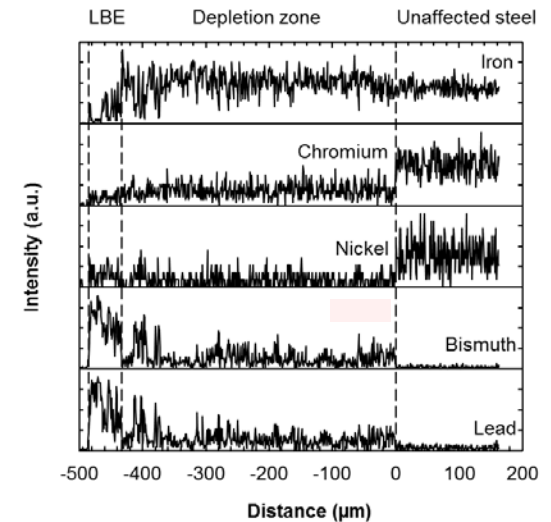
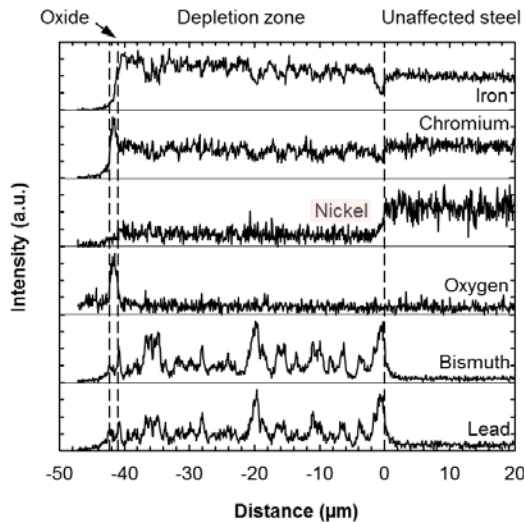
$T = 550^\circ\text{C}$, $v = 2$ m/s, 10^{-6} wt% O

1.4571 after exposure for 5,012 h at 550°C and $c_O \approx 10^{-6}$ wt%



Non-selective leaching (Ni, Cr)

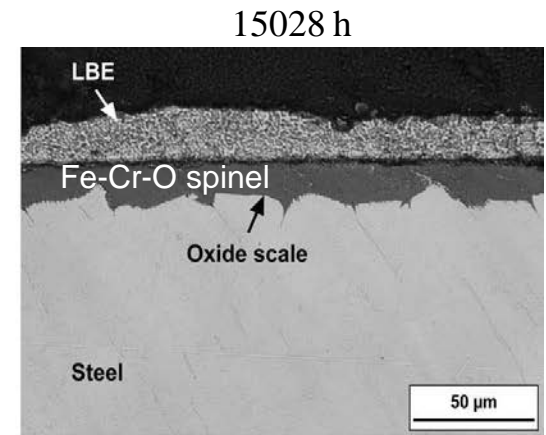
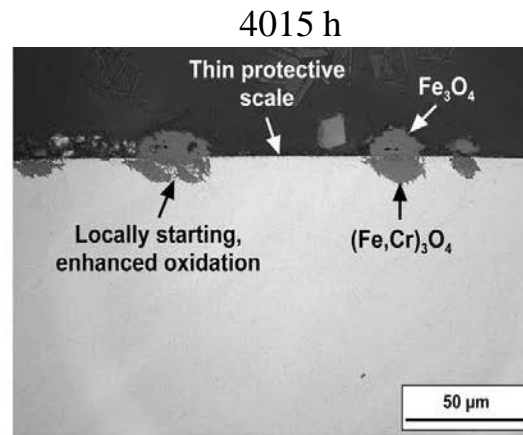
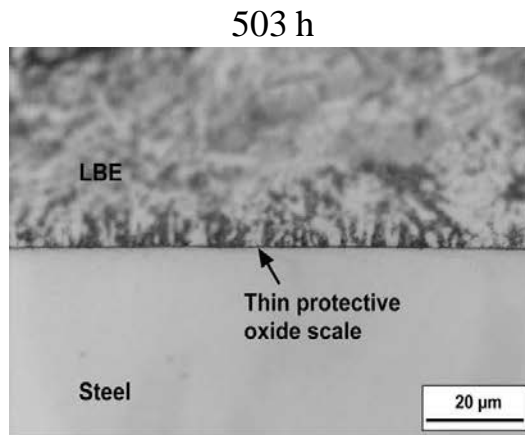
- Starts locally with preferential dissolution of Ni and penetration of Pb and Bi into the depletion zone
- Phase transition from austenite into ferrite resulting from Ni depletion
- Dissolution of Cr after oxygen depletion in the liquid metal penetrating the steel (critical penetration depth)
- In general, insignificant amounts of Cr oxide inside or on the surface of the depletion zone
- Removal of loosened steel grains by the liquid-metal flow in a later stage of severe selective leaching



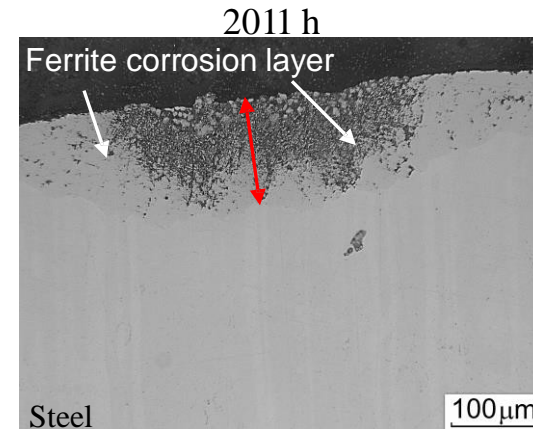
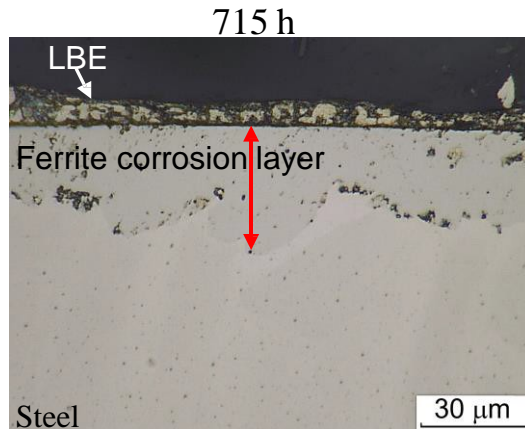
FJOH 2016 Corrosion Phenomena of Austenitic Steels in LBE

General Corrosion Appearance of Austenitic Steel Fe-17Cr-10Ni (316L) at 550°C

10⁻⁶ mass%O



10⁻⁷ mass%O



Ferrite - corrosion layer depleted in Cr and Ni and penetrated by Pb and Bi.

- ❑ At **10⁻⁶ mass%O**, the **oxidation** – main corrosion mode resulted in general material loss of ~18μm (±10) after 15000h;
- ❑ At **10⁻⁷ mass%O** – the **dissolution** is a main corrosion mode resulted in material loss ~51μm (±37) after 2011h.

FJOH 2016 Corrosion Phenomena of Austenitic Steels in LBE

Qualitative Corrosion Appearance of 316L at 450°C depending on Oxygen Concentration

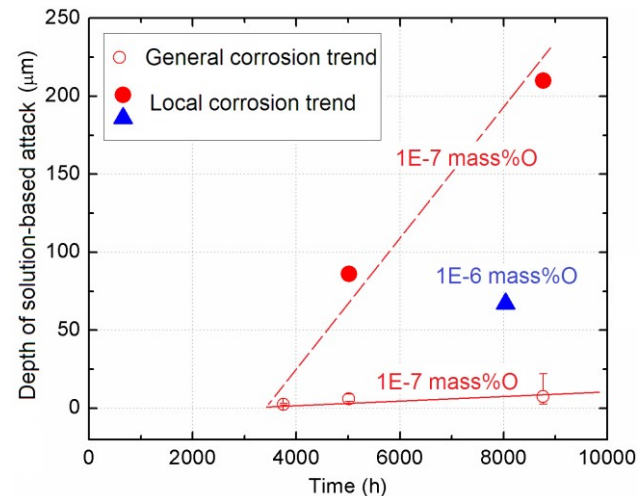
10⁻⁷ mass%O

- ❑ Protective scaling: Cr-based oxide film ≤1μm;
- ❑ Incubation time ~3000h;
- ❑ Solution-based attack resulted in formation of ferrite layer with general material loss of ~8μm (±6) after 8766h;
- ❑ Local corrosion attack with maximum depth of 210μm after 8766h.

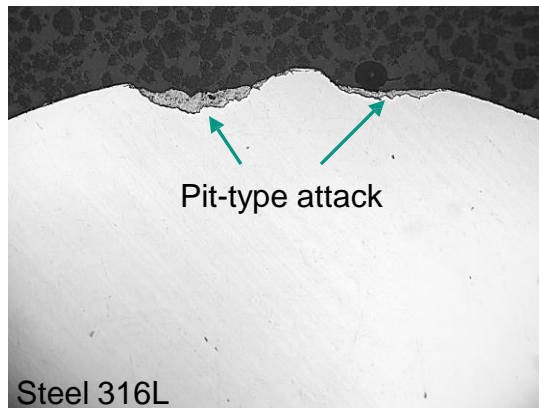
10⁻⁶ mass%O

- ❑ Oxidation: Cr-based oxide and Fe-Cr spinel;
- ❑ Local deep corrosion attack with maximum depth of 67μm after 8039h.
- ❑ Incubation time for local attack is >5000h.

Quantitative output for solution-based corrosion attack

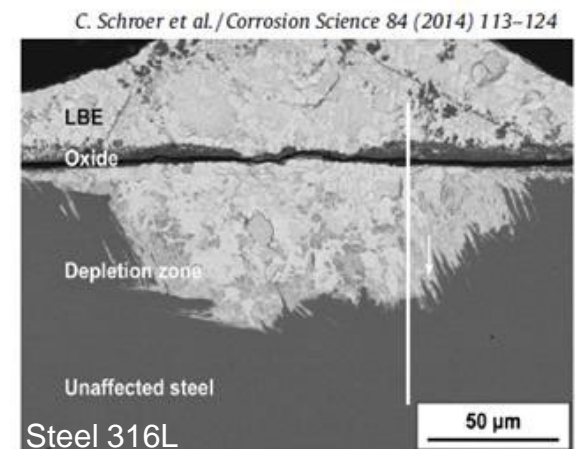


Local corrosion appearance



8766h

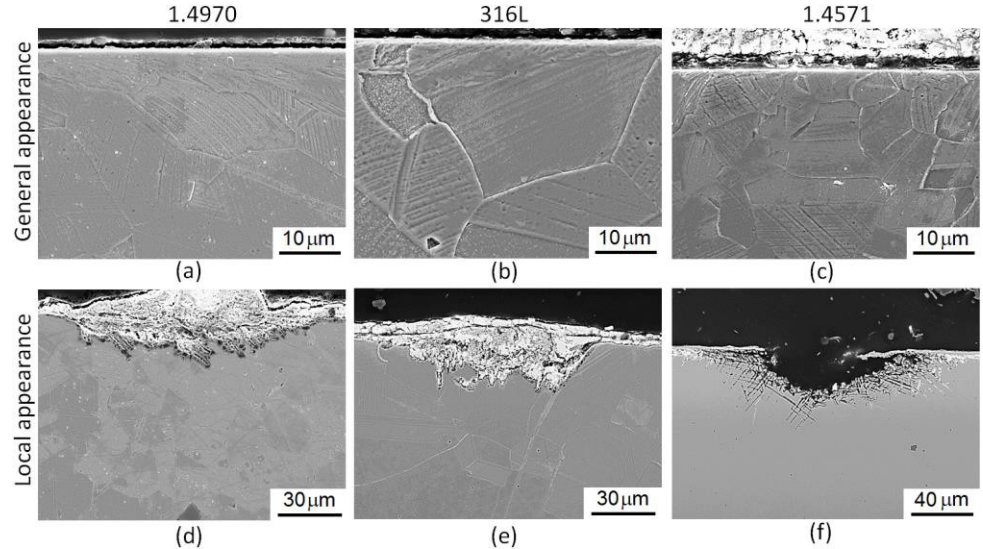
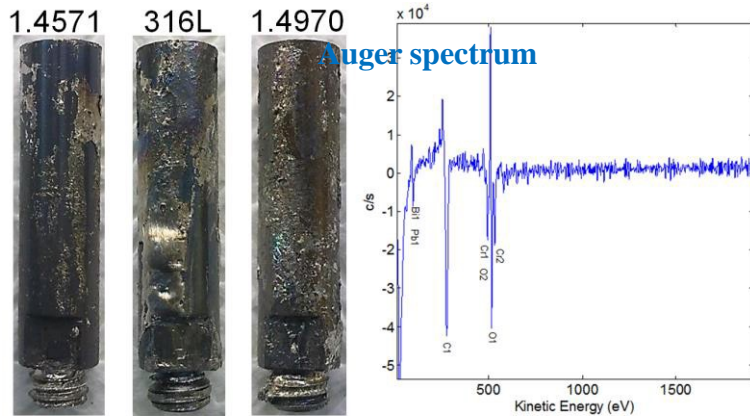
Local corrosion appearance



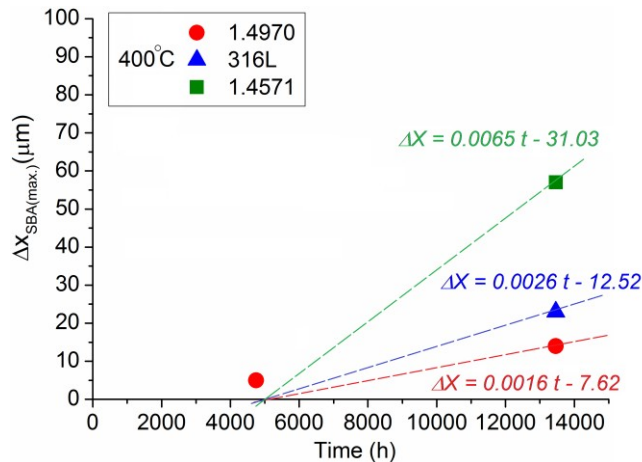
8039h

FJOH 2016 Corrosion Phenomena of Austenitic Steels in LBE

Corrosion Appearance of Austenitic steels at 400°C after 13194 h in Pb-Bi with 10⁻⁷ mass%O



Cr-base oxide film is formed.



Maximum depth of dissolution attack

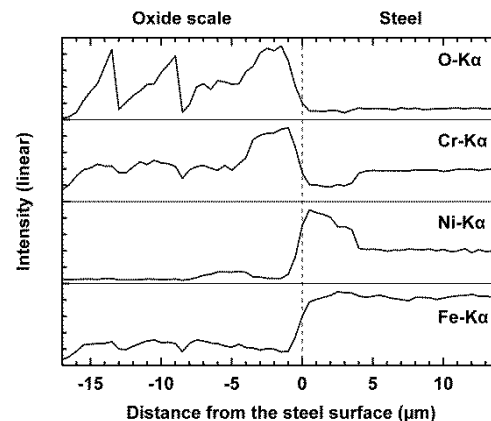
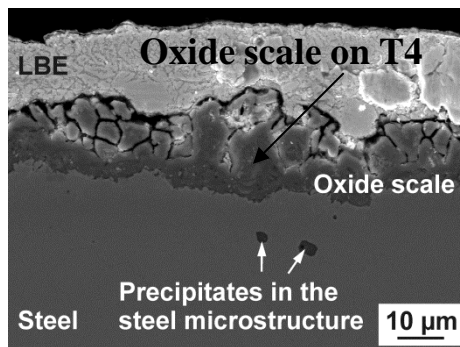
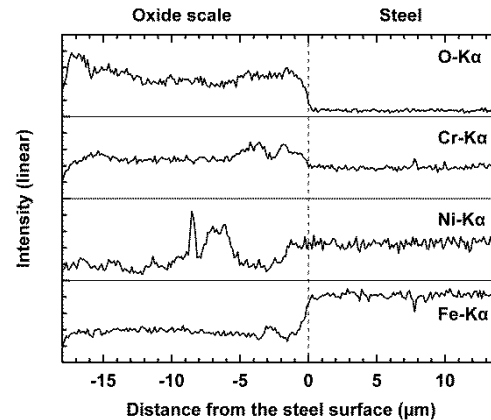
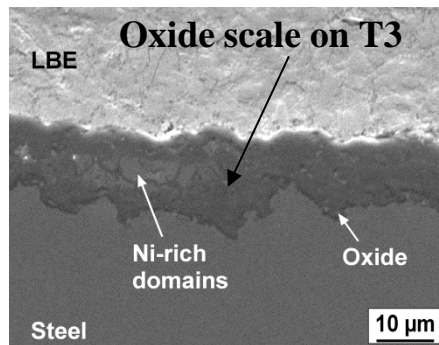
- ❑ Steels show generally good corrosion resistance in Pb-Bi with 10⁻⁷ mass%O for up to 13194 h;
- ❑ Slight general oxidation (Cr-based oxide film) along with very rare local pit-type solution-based corrosion attack are observed;
- ❑ The incubation time for pit-type attack is ~4500 h;
- ❑ After ~13194 h, the maximum pit depth observed was ~ 14, 23 and 57 μm for 1.4970, 316L and 1.4571, respectively;
- ❑ Local corrosion rate ~ 6-26 μm/year.

FJOH 2016 Corrosion Phenomena of Austenitic Steels in LBE

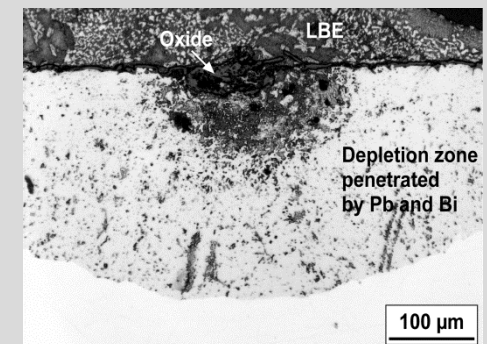
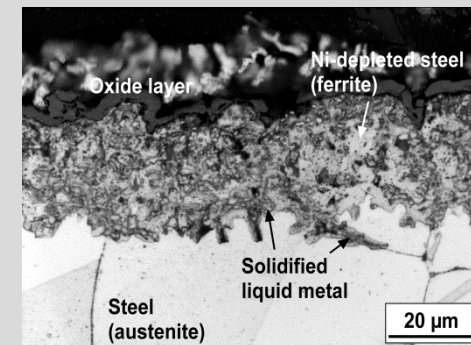
$T = 550^{\circ}\text{C}$, $v = 2 \text{ m/s}$, 10^{-6} wt\% O

Corrosion scales formed in the hot leg (550°C)

- T3 (6000 h) and T4 (40,000 h) mainly show oxidation; T3 was not pre-oxidised
- T1 (23,000 h) and T2 (29,000 h) show significant selective leaching

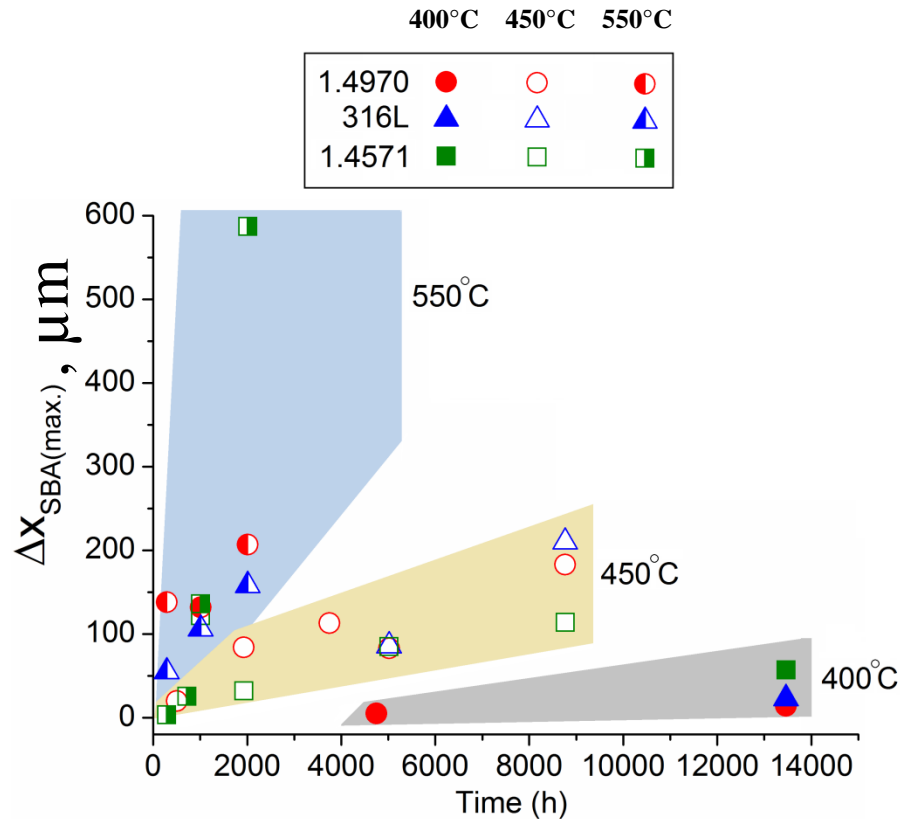


Corrosion scales typically observed on T1 and T2



FJOH 2016 Corrosion Phenomena of Austenitic Steels in LBE

Maximum depth of solution-based corrosion attack observed ($\Delta X_{SBA(max)}$)



Observed corrosion phenomena at:

450 and 550°C:

- ✓ Oxidation – thin Cr-based oxide film;
- ✓ Solution-based corrosion attack – ferrite layer;

In-situ formed oxide film is not a sufficient protective barrier against solution-based corrosion attack at 450 and 550°C.

400°C:

- ✓ Oxidation – thin Cr-based oxide film;
- ✓ Rare local pit-type solution-based corrosion attack;
- ✓ In-situ formed oxide film protects steels against solution-based attack at 400°C.

Maximum corrosion loss:

- ✓ 400°C: 15-60 μm after ~13000 h;
- ✓ 450°C: 120-220 μm after ~9000 h;
- ✓ 550°C: 150-600 μm after ~2000 h.

Incubation time required for initiation of solution-based attack decreases with increasing temperature from about 4500 h at 400°C to ~500 – 4000 h at 450°C and to ≤ 200 h at 550°C.

Thank you for your attention